Science in China Series C: Life Sciences

The guanidine hydrochloride-induced denaturation of CP43 and CP47 studied by terahertz time-domain spectroscopy

QU YuanGang[1,3], CHEN Hua[2], QIN XiaoChun[1], WANG Li[2], LI LiangBi[1†] & KUANG TingYun[1†]

[1] Key Laboratory of Photosynthesis and Environmental Molecular Physiology, Institute of Botany, Chinese Academy of Sciences, Beijing 100093, China;
[2] Laboratory of Optical Physics, Institute of Physics and Center for Condensed Matter Physics, Chinese Academy of Sciences, Beijing 100080, China;
[3] Graduate University of Chinese Academy of Sciences, Beijing 100049, China

Terahertz time-domain spectroscopy (THz-TDS) is a new technique in studying the conformational state of a molecule in recent years. In this work, we reported the first use of THz-TDS to examine the denaturation of two photosynthesis membrane proteins: CP43 and CP47. THz-TDS was proven to be useful in discriminating the different conformational states of given proteins with similar structure and in monitoring the denaturation process of proteins. Upon treatment with guanidine hydrochloride (GuHCl), a 1.8 THz peak appeared for CP47 and free chlorophyll *a* (Chl *a*). This peak was deemed to originate from the interaction between Chl *a* and GuHCl molecules. The Chl *a* molecules in CP47 interacted with GuHCl more easily than those in CP43.

CP43, CP47, guanidine hydrochloride, terahertz time-domain spectroscopy, chlorophyll *a*, collective vibrational modes

CP43 and CP47, the core antenna subunits of photosystem II (PSII), are encoded by the *psb*C and *psb*B genes, respectively, in the chloroplast genome of higher plants and green algae, and in the genomic DNA of cyanobacteria[1−3]. Both CP43 and CP47 have six transmembrane α-helices, which are separated by five extrinsic loop domains[2]. CP43 and CP47 have 473 and 510 amino residues, respectively. CP43 and CP47 bind chlorophyll *a* (Chl *a*) and β-Carotene (β-Car), but not chlorophyll *b* (Chl *b*)[1−3]. CP43 and CP47 can accept excitation energy that is harvested by the light-harvesting complex II (LHC II) and then transfer it directly to the PSII reaction center (RC)[1].

There are many low-frequency collective vibrational modes in biomolecules, such as proteins, DNA, saccharides and other biomolecules. Collective vibrational modes involve the motion of a number of atoms moving in a concerted fashion, and are therefore very sensitive to the conformation and structure of the molecule and its environment. Since the interaction forces are weak and the moving masses are considerably large, the related spectral responses are distributed in the terahertz (THz) region[4−11].

THz radiation lies between the far-infrared (FIR) and microwave regions in the electromagnetic spectrum, with frequencies from 0.1 to 10 THz. The optical characteristics of large biomolecules in the THz range can be obtained by terahertz time-domain spectroscopy (THz-TDS)[12]. THz-TDS was initially developed in the early 1980s[10]. It enabled the direct quantitative detection and conformational analysis of biomolecules[13]. So the use of THz-TDS for studies of conformational flexibility and conformational change in biomolecules has attracted much interest in recent years. Walther et al.

Received August 15, 2006; accepted December 4, 2006
doi: 10.1007/s11427-007-0048-7
†Corresponding authors (email: kuangty@ibcas.ac.cn; lbli@ibcas.ac.cn)
Supported by the National Natural Science Foundation of China (Grant No. 39890390)

measured the far-infrared spectrum of retinal chromophores and found that it could distinguish between different isomeric configurations[9]. Markelz et al. discussed low frequency collective vibrational modes of DNA, bovine serum albumin, and collagen[8]. Furthermore, far-infrared spectra of benzoic acid and its derivatives[14], and of nucleobases of DNA[15] have been reported.

In the previous studies of CP43 and CP47, attention was mainly focused on the electronic spectroscopy of pigments and the secondary structure of the apoprotein[16−21]. Although some articles[22,23] have reported investigation of the vibrational spectroscopy of CP43 and CP47 by resonance Raman spectroscopy, they only presented some vibrational properties of the pigments in the IR band. As for the low-frequency collective vibrational modes of CP43 and CP47 in the THz region, no studies have been conducted as yet. The vibrational spectroscopy of CP43 and CP47 has the potential to answer important questions concerning its structure and function.

In the present study, for the first time, we shed light on the low-frequency collective vibrational spectra of CP43 and CP47 in the THz region by THz-TDS. Their changes induced by guanidine hydrochloride (GuHCl), which has been proved to be the most powerful among commonly used protein denaturants[24], were also studied. It must be pointed out that THz-TDS is an optical technique that can pinpoint the molecular structure without using visible light, thereby avoiding effects like photobleaching in CP43 and CP47, which are light-sensitive materials.

1 Materials and methods

1.1 Purification of CP43 and CP47

CP43 and CP47 were purified from spinach according to the method of Alfonso et al.[18]. The superabundant β-dodecyl maltoside (DM, a mild nonionic detergent) in CP43 preparation was removed by the method of Jankowiak et al.[25]. The CP43 and CP47 samples prepared by these methods already had no membrane, but had DM molecules on the surface of the protein that solubilized the CP43 and CP47 into water. The CP43 and CP47 samples here were the same as those "*in vivo*", which were tested by sodium dodecyl sulfate-polyacrylamide gel electrophoresis (SDS-PAGE), absorption, fluorescence and circular dichroism (CD) spectroscopy.

1.2 GuHCl treatment

The purified CP43 or CP47 was suspended in 20 mmol/L Bis-Tris and 0.05% DM (pH 6.0). The final concentrations of CP43 and CP47 were 3 μg Chl *a* /mL. CP43 and CP47 were incubated in 6 mol/L GuHCl solutions with 20 mmol/L Bis-Tris and 0.05% DM (pH 6.0), and free Chl *a* (obtained from Sigma) was incubated in 6 mol/L GuHCl solutions with 1.25% DM in the dark at room temperature for 6 h.

1.3 Fluorescence spectra

Fluorescence spectra were measured at 77 K by an F-4500 fluorescence spectrophotometer (Hitachi, Tokyo, Japan). Both the excitation and emission band passes were 5.0 nm, and the scan rate was 120 nm/min with a time constant of 2 s.

1.4 THz-TDS

The native or denatured CP43 and CP47 were concentrated to 0.2 mg Chl *a* /mL. Before the THz-TDS measurement, the protein solutions were first mixed with polyethylene (PET) powder. As a nonionic detergent, DM in the protein solutions could facilitate the mixture of protein solutions with PET powder. Since PET is nearly transparent in the THz waveband, it is a suitable filling material for spectroscopic applications in this spectral region. For each sample, 50 μL protein solution was put into 88 mg PET powder that was held in a disk-like cell with high-density polyethylene windows. A thin metallic rod was used to stir the mixture until it was uniformly mixed. Then an electric blower was used to vaporize the moisture in the mixture. Finally, the mixture was compressed into a disk of about 10 mm in diameter and 1.5 mm in thickness. All the THz-TDS measurements were conducted in a vacuum chamber to avoid the interference of water vapor and to insure the sample remaining in dry conditions. For each measurement, a reference waveform was taken by replacing the sample with PET powder mixed with buffer solution (with or without 6 mol/L GuHCl).

A standard THz-TDS configuration was used in our study. The THz radiation was generated by a piece of (100)-oriented InAs wafer, which was excited by optical pulses from a mode-locked Ti-sapphire laser (λ=800 nm, τ_{FWHM} =100 fs). The THz wave was collected and aligned by a pair of paraboloid mirrors before being focused onto the sample. After passing the sample, the THz wave was re-aligned and then detected via the

electro-optic effect in a (110)-oriented ZnTe crystal. All the acquired sample and reference waveforms were converted to their Fourier transforms $E_s(\omega)$ and $E_r(\omega)$, respectively, and the transmission spectra were obtained as a ratio of their Fourier spectra, which was $E_s(\omega)/E_r(\omega)$. The complex system response was simply eliminated in this way. In our experiment, the multi-reflection pulses could be well resolved temporally and therefore, the spectral interference resulting from the etalon effect was ruled out by truncation of the reflected pulses.

2 Results

2.1 Changes of the THz spectra of CP43 and CP47 induced by GuHCl

Figure 1 showed the THz transmission spectra through the GuHCl-denatured CP43 and CP47 as well as the intact ones. The THz transmission spectra through the CP43 and CP47 were almost the same except for a slight decrease of the full width at half-maximum (FWHM) for CP43. After being treated with 6 mol/L GuHCl, for CP43, the spectra shifted significantly to low frequency; for CP47, the spectra had no shift, but a well-resolved peak appeared at around 1.8 THz. For both CP43 and CP47, the FWHM became less.

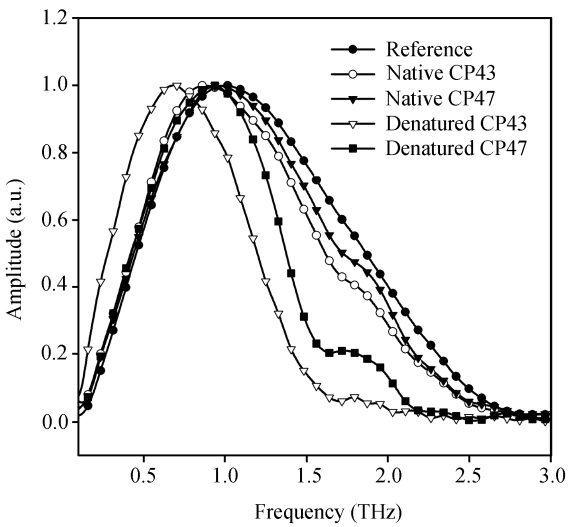

Figure 1 The THz transmission spectra through the CP43 and CP47 with and without the treatment by 6 mol/L GuHCl. The data were normalized to the peak value of the reference spectra.

The absorptance of the samples can be expressed as

$$E_s(\omega)/E_r(\omega) = T(n)\exp(-\alpha d + in\omega d/c),$$

where $T(n)$ is a factor related to the reflection at the sample/PET window interfaces, d is the sample thickness, and c the light velocity in vacuum. Figure 2 showed the THz absorption spectra of the samples. For a better depiction, we divided the THz region we used into three bands: I (0.3－1.5 THz), II (1.5－2.8 THz) and III (2.8－3.5 THz) bands, respectively. In band I, the absorption spectra of CP43 and CP47 were almost similar. In band II, there was a well-resolved peak at 2.4 THz in CP47, which was not apparent in CP43. In band III, there was only a peak at 3.28 THz for CP43, but for CP47 there were three peaks. Both CP43 and CP47 had broadband THz absorption, suggesting that a large density of low-frequency collective vibrational modes is indeed THz active. After treatment with 6 mol/L GuHCl, in band I, the absorbance increased rapidly with increasing frequency for both CP43 and CP47, and the slope of CP43 exceeded that of CP47. In band II, instead of three well-resolved peaks in CP47, a wide absorbance platform appeared in CP43. In band III, though there were two peaks for both CP43 and CP47, the relative intensity of the two peaks in CP43 differed from those of CP47.

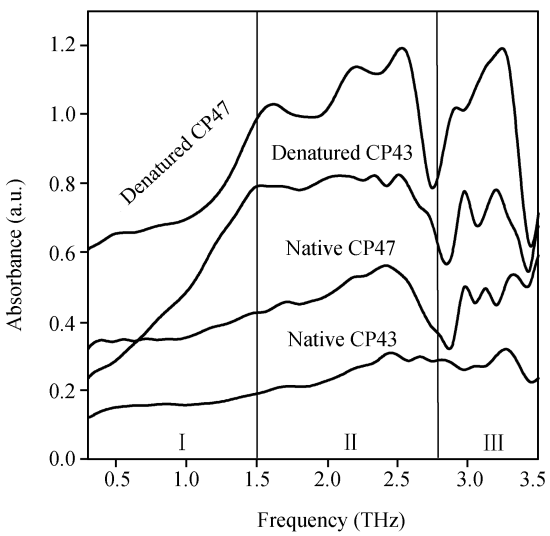

Figure 2 The THz absorption spectra of the CP43 and CP47 with and without the treatment by 6 mol/L GuHCl (drawn with an offset for better representation).

It should be noted that the buffer we used (with or without 6 mol/L GuHCl) had no apparent THz signal (data not shown). In addition, after GuHCl treatment, no pigments were dissociated from CP43 and CP47, which could be verified by ultracentrifugation. These results suggested that the THz spectra of CP43 and CP47 presented here were the signal of CP43 and CP47 themselves but not the buffer or the dissociated Chl *a*

molecules in buffer.

2.2 Changes of the THz transmission spectra through the free Chl *a* induced by GuHCl

To probe the origin of the 1.8 THz peak for CP47, we measured the changes of the THz transmission spectra through the free Chl *a* induced by GuHCl. After treatment with 6 mol/L GuHCl, though the THz transmission spectra of free Chl *a* had no shifts and the FWHM also had no apparent changes, a well-resolved peak around 1.8 THz appeared (Figure 3), which was similar to that of CP47 but not to that of CP43.

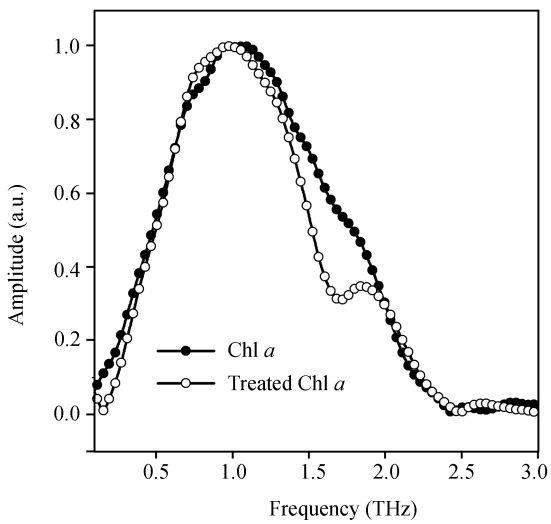

Figure 3 The THz transmission spectra through the free Chl *a* with and without the treatment by 6 mol/L GuHCl. The data were normalized to the peak value of the free Chl *a* spectra.

2.3 Changes of the fluorescence emission spectra of Chl *a* in CP43 and CP47 induced by GuHCl

In this study, 436 nm light, an absorption maximum of Chl *a* in CP43 and CP47, was used to excite Chl *a*. As shown in Figure 4, upon excitation at 436 nm, the fluorescence emission peaks of CP43 and CP47 were at 681 and 693 nm, respectively. The fluorescence intensity of both CP43 and CP47 decreased after treatment with 6 mol/L GuHCl. However, the fluorescence intensity of CP47 decreased more than that of CP43. In addition, the fluorescence peak of CP47 shifted to the blue region, whereas that of CP43 had no obvious shift.

3 Discussion

There is an increasing interest in the collective vibrational modes occurring in proteins, as these modes may provide information about a protein's conformational state[10]. Although the secondary and tertiary structures of native CP43 and CP47 are very similar[1−3], the THz spectra, particularly the THz absorption spectra, of the native CP43 and CP47 were different (Figures 1 and 2). This illustrated that THz-TDS was sensitive in discriminating the different conformational states of proteins with similar structure. After treatment with GuHCl, the THz transmission spectra and the THz absorption spectra of CP43 and CP47 both changed, and the changes of CP43 and CP47 were different (Figures 1 and 2). This indicated that the low-frequency collective vibrational modes of CP43 and CP47 changed by GuHCl, and the changes were different. This further implied that the denatured CP43 and CP47 were in different unfolding states. Our previous study also showed that, after treatment with GuHCl, the secondary and tertiary structure of CP43 and CP47 both changed and the changes between CP43 and CP47 were different[26]. All the above results demonstrated that THz-TDS could be applied to monitoring the denaturation process of photosynthesis membrane proteins.

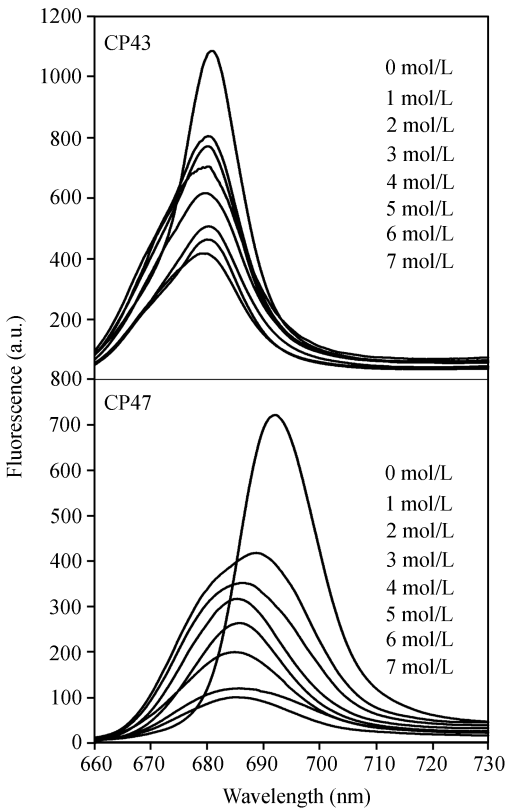

Figure 4 The 77 K fluorescence emission spectra of the CP43 and CP47 excited at 436 nm after treatments with different concentrations of GuHCl. The GuHCl concentration from top to bottom was 0−7 mol/L, respectively.

The previous study[27] provided direct evidence that GuHCl interacted with proteins by multiple hydrogen-bonding interactions. The binding of GuHCl involves both the protein side-chain and backbone atoms, and no particular type of amino acid appears to be a preferential target for denaturation binding. Some other studies[14,28] showed that low-frequency vibrations, typically between 0.5 and 6 THz, originated from not only the internal motions but also the intermolecular modes (e.g., vibrations and torsions of intermolecular hydrogen bonds). For free Chl *a*, a well-resolved peak around 1.8 THz appeared in the THz transmission spectra after being treated with GuHCl (Figure 3). Considering the interaction form between the protein and GuHCl molecule, we inferred that this peak might result from the hydrogen bonds that occurred between the C═O group of the Chl *a* molecule and the NH group of the GuHCl molecule. For BSA, which contained no Chl *a*, no 1.8 THz peak appeared when being treated with GuHCl (data not shown). This also confirmed our conjecture from another point of view.

Upon a treatment with GuHCl, a 1.8 THz peak appeared in CP47 but was not apparent in CP43 (Figure 1). Based on the above view, it indicated that chlorophyll molecules in CP47 interacted with GuHCl more easily than those in CP43.

In order to further study how GuHCl affected the Chl *a* molecules in CP43 and CP47, we measured Chl *a* fluorescence emission spectra of CP43 and CP47. After being treated with GuHCl, the decrease of the fluorescence intensity of CP43 and CP47 (Figure 4) indicated changes of the Chl *a* chromophores. In comparison with CP43, the greater decrease of the fluorescence intensity of CP47 and its manifest blue shift of the peak position (Figure 4) implied a greater change of its Chl *a*. In other words, GuHCl disturbed Chl *a* in CP47 more than that in CP43. This was consistent with the results obtained from the THz spectra. The reason for this might be related to the fact that the apoprotein of CP43 could protect Chl *a* more effectively than that of CP47, because the apoprotein structure of CP43 was less sensitive to GuHCl than that of CP47[26].

In conclusion, THz-TDS was proven to be useful in discriminating the different conformational states of given proteins with similar structure and in monitoring the denaturation process of proteins. Upon a treatment with GuHCl, the 1.8 THz peak was deemed to originate from the interaction between Chl *a* and GuHCl molecules. The Chl *a* molecules in CP47 interacted with GuHCl more easily than those in CP43.

1 Bricker T M. The structure and function of CP-1 and CP-2 in photosystem II. Photosynth Res, 1990, 24: 1－13

2 Bricker T M, Frankel L K. The structure and function of CP47 and CP43 in photosystem II. Photosynth Res, 2002, 72: 131－146

3 Barber J, Morris E, Büchel C. Revealing the structure of the photosystem II chlorophyll binding proteins, CP43 and CP47. Biochim Biophys Acta, 2000, 1459: 239－247

4 Walther M, Fischer B M, Jepsen P U. Noncovalent intermolecular forces in polycrystalline and amorphous saccharides in the far infrared. Chem Phys, 2003, 288: 261–268

5 Fischer B M, Walther M, Jepsen P U. Far-infrared vibrational modes of DNA components studied by terahertz time-domain spectroscopy. Phys Med Biol, 2002, 47: 3807－3814

6 Nishizawa J, Suto K, Sasaki T, et al. Spectral measurement of terahertz vibrations of biomolecules using a Gap terahertz-wave generator with automatic scanning control. J Phys, 2003, 36: 2958－2961

7 Shen Y C, Upadhya P C, Linfield E H, et al. Temperature-dependent low-frequency vibrational spectra of purine and adenine. Appl Phys Lett, 2003, 82: 2350－2352

8 Markelz A G, Roitberg A, Heilweil E J. Pulsed terahertz spectroscopy of DNA, bovine serum albumin and collagen between 0.1 and 2.0 THz. Chem Phys Lett, 2000, 320: 42－48

9 Walther M, Fischer B, Schall M, et al. Far-infrared vibrational spectra of all-trans, 9-cis and 13-cis retinal measured by THz time-domain spectroscopy. Chem Phys Lett, 2000, 332: 389－395

10 Smye S W, Chamberlain J M, Fitzgerald A J, et al. The interaction between terahertz radiation and biological tissue. Phys Med Biol, 2001, 46: R101－R112

11 Markelz A, Whitmire S, Hillebrecht J, et al.. THz time domain spectroscopy of biomolecular conformational modes. Phys Med Biol, 2002, 47: 3797－3805

12 Wang W N, Yue W W, Yan H T, et al. THz time-domain spectroscopy of amino acids. Chin Sci Bull, 2005, 50(15): 1561－1565

13 Upadhyal P C, Shen Y C, Davies A G, et al. Terahertz time-domain spectroscopy of glucose and uric acid. J Biol Phys, 2003, 29: 117－121

14 Walther M, Plochocka P, Fischer B, et al. Collective vibrational modes in biological molecules investigated by terahertz time-domain spectroscopy. Biopolymers, 2002, 67: 310－313

15 Fischer B, Walther M, Jepsen P Uhd. Far-infrared spectroscopy of hydrogen bonding in nucleobases, nucleosides, and nucleotides. In: Chamberlain J M, ed. Proc. of 2002 IEEE 10th International Conference on Terahertz Electronics, Cambridge, 2002. Piscataway: IEEE, 2002. 74－76

16 Guo S K, Tang C Q, Yang Z L, et al. Effects of acid and alkali on the light absorption, energy transfer and protein secondary structures of core antenna subunits CP43 and CP47 of Photosystem II. Photochem Photobiol, 2004, 79: 291－296
17 Wang J S, Shan J X, Xu Q, et al. Light- and heat-induced denaturation of photosystem II core-antenna complexes CP43 and CP47. J Photochem Photobiol, 1999, 50: 189－196
18 Alfonson M, Montoya G, Cases R, et al. Core antenna complexes, CP43 and CP47, of higher plant photosystem II. Spectral properties, pigment stoichiometry, and amino acid composition. Biochemistry, 1994, 33: 10494－10500
19 Shan J X, Wang J S, Ruan X, et al. Changes of absorption spectra during heat-induced denaturation of photosystem II core antenna complexes CP43 and CP47: revealing the binding states of chlorophyll molecules in these two complexes. Biochim Biophys Acta, 2001, 1504: 396－408
20 Groot M L, Peterman E J, van Stokkum I H, et al. Triplet and fluorescing states of the CP47 antenna complex of photosystem II studied as a function of temperature. Biophys J, 1995, 68: 281－290
21 Weerd F L De, van Stokkum I H M, van Amerongen H, et al. Pathways for energy transfer in the core light-harvesting complexes CP43 and CP47 of photosystem II. Biophys J, 2002, 82: 1586－1597
22 Shan J X, Yang K Y, Feng L J, et al. Resonance Raman spectra of purified PSII core antenna complexes CP43 and CP47. Acta Bot Sin, 1999, 41: 280－284
23 De Paula J C, Liefshitz A, Hinsley S, et al. Structure-function relationship in the 47-kDa antenna protein and its complex fluorescence decay kinetics and resonance Raman spectroscopy. Biochemistry, 1994, 33: 1455－1466
24 Nozaki Y. The preparation of guanidine hydrochloride. Methods Enzymol, 1972, 26: 43－51
25 Jankowiak R, Zazubovich V, Rätsep M, et al. The CP43 core antenna complex of photosystem II possesses two quasi-degenerate and weakly coupled Qy-trap states. J Phys Chem, 2000, 104: 11805－11815
26 Qu Y G, Gong Y D, Guo S K, et al. Structural characteristics of extra-membrane domains and guanidine hydrochloride-induced denaturation of photosystem 2 core antenna complexes CP43 and CP47. Photosynthetica, 2006, 44: 447－453
27 Dunbar J, Yennawar H P, Banerjee S, et al. The effect of denaturants on protein structure. Protein Sci, 1997, 6: 1727－1733
28 Korter T M, Balu R, Campbell M B, et al. Terahertz spectroscopy of solid serine and cysteine. Chem Phys Lett, 2006, 418: 65－70